Geophysical Research Letters

RESEARCH LETTER
10.1029/2024GL109777

Deciphering the Prevalence of Warm-Wet Extremes in Ice-Covered Zones

Xinlu Chen[1,2], Lianlian Xu[1,2], Ran Yang[1], Ming Cai[3], Yi Deng[4], Deliang Chen[5], Song Yang[1,2], Jiping Liu[1], Qinghua Yang[1], and Xiaoming Hu[1,2]

[1]School of Atmospheric Sciences, Sun Yat-sen University and Southern Marine Science and Engineering Guangdong Laboratory (Zhuhai), Zhuhai, China, [2]Guangdong Province Key Laboratory for Climate Change and Natural Disaster Studies, Zhuhai, China, [3]Department of Earth, Ocean and Atmospheric Sciences, Florida State University, Tallahassee, FL, USA, [4]School of Earth and Atmospheric Sciences, Georgia Institute of Technology, Atlanta, GA, USA, [5]Regional Climate Group, Department of Earth Sciences, University of Gothenburg, Gothenburg, Sweden

Key Points:

- In contrast to midlatitude regions where warm-dry extremes are common, warm-wet extremes prevail over polar regions
- Poleward circulation associated with high pressure systems, rather than subsidence, produces warm-wet conditions
- Snow- and ice-covered surfaces neutralize the land-air interaction feedback loop that reinforces hot-dry spells in midlatitude regions

Correspondence to:
X. Hu,
huxm6@mail.sysu.edu.cn

Citation:
Chen, X., Xu, L., Yang, R., Cai, M., Deng, Y., Chen, D., et al. (2024). Deciphering the prevalence of warm-wet extremes in ice-covered zones. *Geophysical Research Letters*, *51*, e2024GL109777. https://doi.org/10.1029/2024GL109777

Received 13 APR 2024
Accepted 28 AUG 2024

Abstract Compound warm extremes exert profound impacts on environment, health, and socioeconomics. Yang et al. (2024) indicated a shift or transition from warm-dry extremes (WDEs), common in non-ice-covered areas, to warm-wet extremes (WWEs) in ice-covered zones. Utilizing ERA5 reanalysis data, this study determined the duration and frequency of WDEs and WWEs across ice-covered and non-ice-covered regions. A comprehensive analysis uncovers the physical mechanisms responsible for the paradigm differences and attributes them to the weakening of land-atmosphere interaction caused by ice-cover, which inhibits soil moisture feedback and reduces the intensity and duration of warm events in ice-covered areas. Both WDEs and WWEs are associated with high-pressure systems (HPs). WDEs, situated directly beneath HPs, intensify due to adiabatic warming from subsidence motions. Conversely, WWEs, located beneath the poleward fringes of HPs, emerge from advective warming and moistening associated with poleward intrusions of warm-moist air.

Plain Language Summary Significantly rising temperatures can coincide with extreme weather events such as droughts or rainstorms to form compound warm-dry extremes (WDEs) or warm-wet extremes (WWEs), leading to more severe consequences than just hot weather alone. Recent findings indicate that WDEs are more prevalent in non-ice-covered regions where people reside and crops are cultivated, while WWEs are more common in ice-covered areas. This study seeks to comprehend the reasons behind the paradigm differences of extreme events by analyzing the conditions during hot summers. Our research has identified two primary causes for the paradigm differences. First, in non-ice-covered regions, the ground warms the overlying air, which in turn dries out the soil, leading to even higher temperatures. This explains why more WDEs are observed in these areas. However, in ice-covered regions, this process is inhibited by ice. Second, the high-pressure systems accompanying these extreme events behave differently based on the presence or absence of ice. In non-ice-covered regions, these systems are located directly above the regions, exacerbating the hot-dry conditions by pushing air downwards. Conversely, hot-wet conditions occur in ice-covered regions because these areas are situated beneath the poleward fringes of the systems, which transport warm and moist air from the lower latitudes.

1. Introduction

In recent years, extreme high temperatures have often been observed to coincide with other extremes such as heavy precipitation and droughts, and these compound extremes have received increasing attention due to their more significant environmental and societal impacts compared to separate extremes (Feng et al., 2019; Ridder et al., 2020). The prevalence of compound warm-dry extremes in populated and cropland areas, as well as their impacts (e.g., public health risks, energy crisis, wildfires, etc.), has been discussed extensively in studies at both regional and global scales (Afroz et al., 2023; Hao et al., 2018; Holmes et al., 2017; Liu & Zhou, 2023a, 2023b; Mueller & Seneviratne, 2012; Salvador et al., 2023; Xu et al., 2023; Zscheischler & Seneviratne, 2017). However, there has been less focus on compound warm extremes over polar ice sheets. Different from the predominant synchronization of extreme warm and dry conditions in midlatitude environments, extreme high temperatures over polar ice sheets tend to co-occur with precipitation, which have been observed in West Antarctica (Djoumna & Holland, 2021; Nicolas & Bromwich, 2011), Antarctic Peninsula (Gorodetskaya et al., 2023), East Antarctica (Clem et al., 2023), and Greenland (Mattingly et al., 2020; Xu et al., 2022).

In contrast to the direct effect induced by warm-dry spells on midlatitude lands, warm-wet extremes over polar ice sheets may lead to more complex and profound climate impacts. These warm and wet conditions can amplify the vulnerability of ice sheets through triggering extensive surface melt, leading to destabilization of coastal ice, significant ice mass loss, and freshwater inflow into the oceans (Bell et al., 2018; Hu et al., 2019; Stokes et al., 2022). Ultimately, these processes contribute to accelerated sea level rise (DeConto & Pollard, 2016; Rignot et al., 2011) and weakened Atlantic Meridional Overturning Circulation (Bakker et al., 2016; Gao et al., 2024; Zhu et al., 2014). Given the significant impact of warm-wet extremes on ice-covered regions, Yang, Hu, et al. (2024) pointed out that these areas exhibit a much higher synchrony of extreme warm and precipitation events compared to the midlatitude lands, suggesting paradigm differences of compound warm extremes between non-ice covered regions and ice-covered regions. This synchrony may arise from warm-moist air intrusions discussed by previous studies over Greenland (Barrett et al., 2020; Bintanja et al., 2023; Pettersen et al., 2022; Ward et al., 2020) and Antarctica (Gorodetskaya et al., 2023; Shields et al., 2022; Wang et al., 2023; Wille et al., 2024).

Systematic studies of the new characteristics and physical mechanisms for compound warm-wet extremes over ice sheets are also crucial under global climate change. On the one hand, the frequency, duration, and intensity of warm extremes has increased (Barriopedro et al., 2023; Feron et al., 2021; González-Herrero et al., 2022); on the other hand, precipitation process tends to shift from a solid state to a liquid state (Bennartz et al., 2013; Schot et al., 2023; Vignon et al., 2021). The combined effect of these two factors could result in a nonlinearly enhanced surface melt on ice caps (Bintanja, 2018; McNeall et al., 2011). While the individual mechanisms associated with compound warm-dry extremes have been widely explored, spanning from local processes (Libonati et al., 2022; Miralles et al., 2019; Zhang et al., 2020) to large-scale modes of climate variability (Jiang et al., 2024; Mukherjee et al., 2020; Yang, Shen, et al., 2024, Yang, Zeng, et al., 2024), there is still a lack of systematic analysis of the compound warm-wet extremes. Moreover, an enhanced understanding of the warm-wet extremes over polar ice sheets contributes to better identifying the model biases in numerical simulations and improving model simulations and thus forecast performance (Cai et al., 2024; Ridder et al., 2021), especially over the cryosphere due to scarce observations and complex dynamics (Deb et al., 2016; Leeson et al., 2018).

As we mentioned previously, Yang, Hu, et al. (2024) highlighted the prevalence of warm-wet extremes over polar regions, which is different from the dominance of warm-dry extremes over the midlatitudes. This study, building upon the perspectives proposed by Yang, Hu, et al. (2024), is aimed to provide robust evidence and physical interpretations for the paradigm differences of compound warm extremes. First, we examine the percentages and duration of WWEs and WDEs during summers from 1979 to 2022 in five representative regions: (a) Greenland and (b) West Antarctica, which are marked by ice-covered surface and have suffered massive surface melt under warm and wet conditions (Dou et al., 2023; Li et al., 2023); (c) Europe, (d) South China, and (e) the US Great Plains, which are identified as the hotspots of research on severe heatwaves and droughts with regard to human health risk and yield loss (Han et al., 2022; He et al., 2022; Tripathy & Mishra, 2023; Zhang et al., 2023). Second, we investigate the relative atmospheric processes and surface energy budget through a composite analysis. The associated land-air interaction is quantified by using a coupling metric (Miralles et al., 2012; Seo & Ha, 2022) to provide an improved understanding of the crucial role in triggering the different compound warm extremes.

2. Data and Methods

2.1. Data

Daily averaged ERA5 reanalysis fields for the summers of 1979–2022 (i.e., June, July, and August for the Northern Hemisphere, and December, January, and February for the Southern Hemisphere) with a horizontal resolution of $1° \times 1°$ are used in this study. The daily averages are calculated from the hourly ERA5 reanalysis data provided by the European Center for Medium-range Weather Forecasts (Hersbach et al., 2020). The surface variables include 2 m temperature (T), total precipitation (P), surface pressure, total cloud cover, integrated moisture flux (IVT), actual and potential evaporation, soil water, sensible and latent heat fluxes, as well as net and downward fluxes of shortwave radiation (SWR) and longwave radiation (LWR). Positive (Negative) values of radiation and heat fluxes in ERA5 are directed downwards (upwards), while positive (negative) values of meridional water vapor flux indicate northward (southward) moisture transport. Geopotential height with a vertical resolution of 10 pressure levels extending from 1000 hPa to 200 hPa are also analyzed.

2.2. Definitions of Compound Extremes

The 75th and 25th percentiles of summer daily T and P from 1981 to 2010 are chosen as the thresholds for extremes, denoted as T_{75}, P_{75}, and P_{25}, respectively. These percentiles allow a larger number of events to be selected for analysis (Beniston, 2009). The co-occurrence of heatwaves ($T > T_{75}$) and extreme precipitation ($P > P_{75}$) is defined as warm-wet extremes (WWEs) at each grid, while the co-occurrence of heatwaves and extreme droughts ($P < P_{25}$) is defined as warm-dry extremes (WDEs). To identify WWEs or WDEs within an area, we first assign one to the land grids where events occur and zero to those where non-events occur on a given day (ocean grids are masked), and then calculate the regional means. Subsequently, a daily time series of the spatial extent of events (i.e., percentage of gridpoints within a defined area that depict an event of interest) within a study region, as well as the standard deviation of the spatial extent calculated from this time series, is obtained. The days when the anomalous spatial extent exceeds one standard deviation are defined as extreme cases. To further explore the mechanisms driving WWEs and WDEs, a composite analysis is applied to the extreme cases. The 95% confidence levels for the WWEs or WDEs composite values deviated from the climatology (i.e., averages over entire period from 1979 to 2022) are determined by the Student's t-test.

2.3. Coupling Metric

Land-atmosphere interactions, whose role in triggering or amplifying warm extremes has been highlighted in previous studies (Hao et al., 2022; Miralles et al., 2014, 2019; Zhang et al., 2023), can be briefly described as a feedback loop: when surface dryness is exacerbated by increasing atmospheric demand of water under anomalously warm conditions, evaporation and its surface cooling effect progressively decline, leading to an accumulation of sensible heat in the atmosphere and to decreases in the likelihood of precipitation that further exacerbates the existing hotness and dryness. To quantify the strength of land-atmosphere interaction at a given location, a coupling metric (π) related to surface energy flux anomalies and their skill in explaining the variation of temperature (T) was proposed by Miralles et al. (2012) as:

$$\pi = \left[(R_n - \lambda E)' - (R_n - \lambda E_p)'\right] \times T' \quad (1)$$

where R_n refers to the surface net radiation, λ is the latent heat of vapourization, and E and E_p denote actual and potential evaporation, respectively. The primes denote the standardized anomalies deviated from the climatology defined in Section 2.2. The energy term (i.e., $\left[(R_n - \lambda E)' - (R_n - \lambda E_p)'\right]$) denotes the contribution of surface moisture deficiency to sensible heat flux anomalies. This term will be zero when surface moisture is sufficient to meet the atmospheric demand, and it increases under dry conditions. Positive values of π are obtained in regions where surface dryness can significantly contribute to extremely atmospheric warming through its effect on local energy balance.

3. Results

3.1. Percentages and Duration of WWEs and WDEs

Figure 1a presents the global pattern of the percentages of WWEs days to the total number of WWEs and WDEs days, illustrating the prevalence of compound warm extremes in summer. The percentages of WWEs exceed 80% over portions of the polar ice sheets but falls below 20% over most midlatitude regions. This result indicates paradigm differences of compound extremes between non-ice-covered zones, where WDEs prevail, and ice-covered regions, where WWEs are common. We explore and compare the mechanisms for WWEs and WDEs, focusing on two regions where WWEs prevail, including Greenland (GL) and West Antarctica (WA), as well as three zones dominated by typical WDEs, including Europe (EU), South China (SC) and the US Great Plains (USGP).

Figure 1b shows the duration of WWEs and WDEs in the above five regions. Short-duration extremes lasting up to 5 days account for more than 75% of both WWEs and WDEs, meaning that these two types of extremes are predominantly short-duration events. There are a few cases that last more than 10 days, particularly over EU. Overall, WDEs last longer than WWEs. Specifically, GL and WA WWEs last less than 10 days, while some WDEs in EU, SC, and USGP persist up to 15 days. In the following sections, we focus on the physical

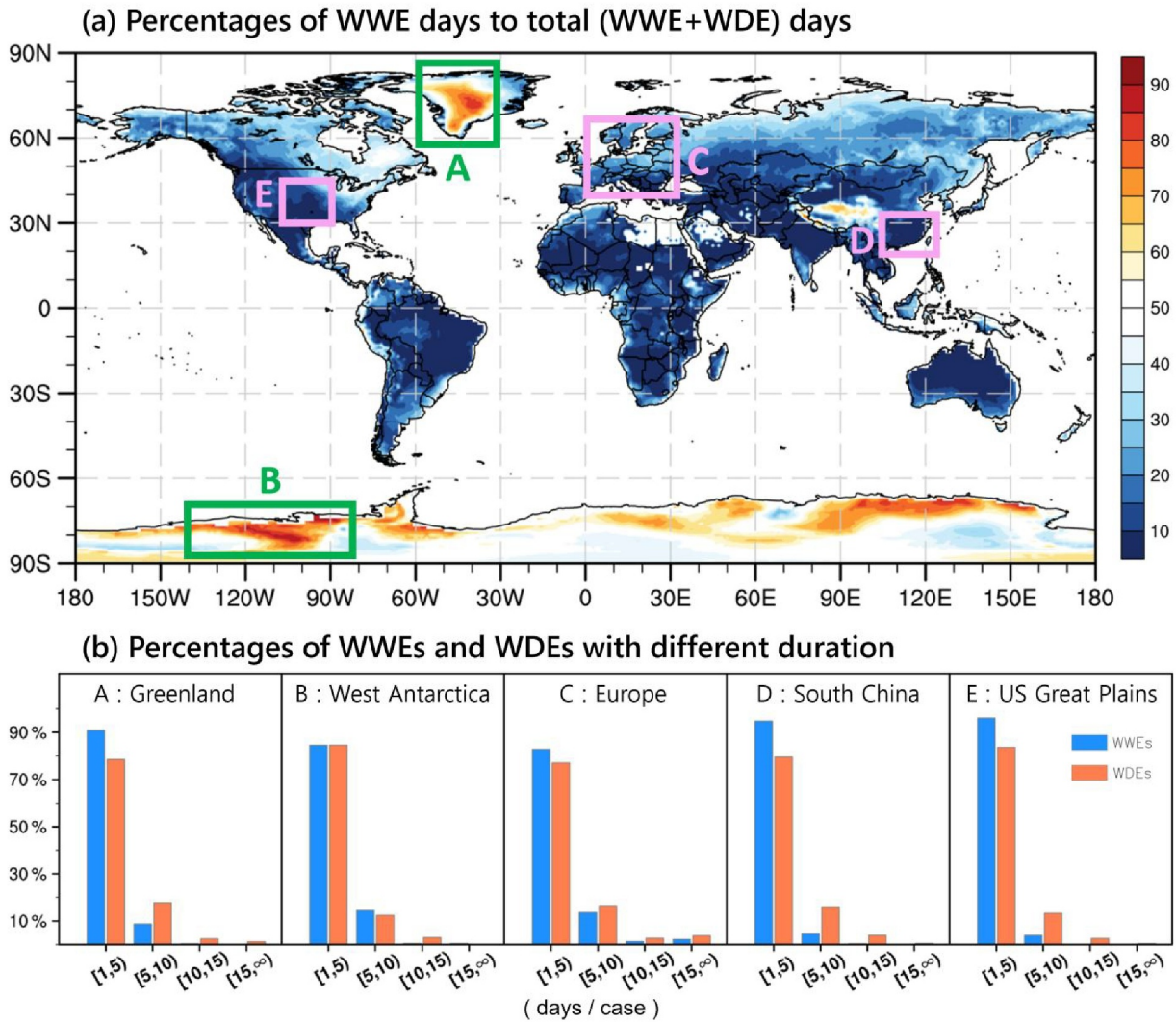

Figure 1. (a) Percentages of warm-wet extreme (WWE) days to the total number of WWE and warm-dry extreme (WDE) days during summer. (b) Percentages of WWEs (WDEs) with different durations in all WWEs (WDEs) in five regions. The regions labeled A, B, C, D, and E in (a) represent Greenland (GL), West Antarctica (WA), Europe (EU), South China (SC), and the US Great Plains (USGP), respectively. The percentages of WWEs (WDEs) in (b) are represented by blue (orange) bars.

mechanisms of the prevalent type of compound warm extremes in each region, namely WWEs in GL and WA but WDEs in EU, SC and USGP.

3.2. Atmospheric Processes and Surface Energy Budget

By definition, near-surface warming during WWEs in GL and WA occurs in conjunction with increased precipitation. This does not occur during WDEs in EU, SC and USGP (Figure 2). During WWEs, robust high-pressure systems (HPs) with a quasi-barotropic vertical structure occur over both GL and WA (Figures 2u and 2v), and the locations of WWEs, indicated by purple lines, are at the poleward fringes of HPs. The Greenland HP is similar to southern Greenland blocking discussed by Pettersen et al. (2022) and Ward et al. (2020), while the West Antarctic HP resembles the Antarctic Peninsula blocking studied by Bozkurt et al. (2022). Guided by the poleward circulation associated with anticyclones, large amounts of heat and moisture from the lower latitudes are transported toward the ice sheets (Figures 2p–2t). As discussed by previous studies (Pettersen et al., 2022; Ward et al., 2020; Zou et al., 2021), these warm-moist air intrusions result in inland warming and, coupled with local elevated elevation, lead to cloud formation (Figures 2k and 2l) and precipitation (Figures 2f and 2g). In the areas where cloud cover increases, downwelling SWR at the surface decreases (Figures 3k and 3l). However, downward LWR is greatly enhanced, amplifying surface warming over the ice-covered surface (Figures 3p and 3q).

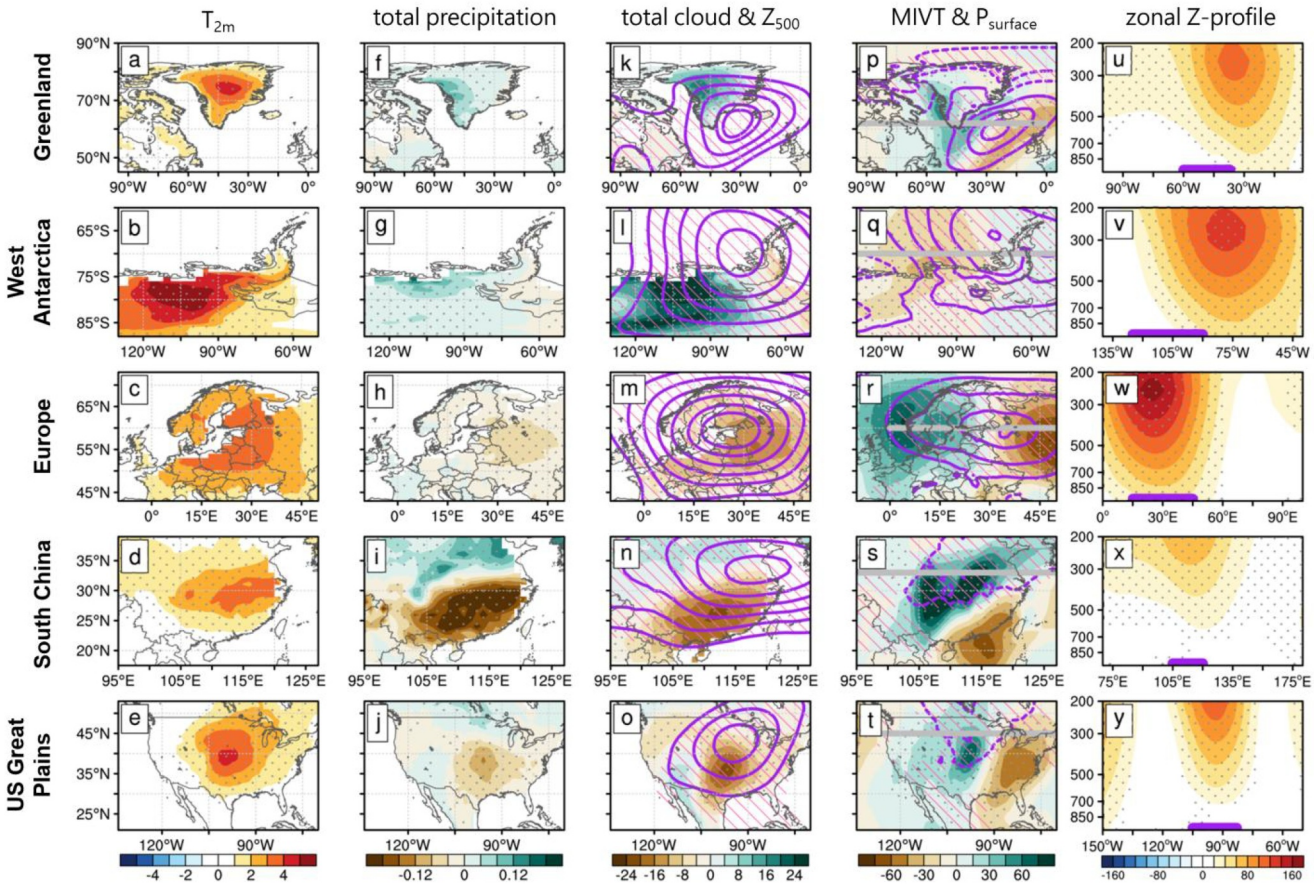

Figure 2. Atmospheric variables associated with the WWEs in GL and WA, and the WDEs in EU, SC and USGP. Shading represents daily composite anomaly values of (a–e) 2 m temperature (units: K) (f–j) total precipitation (units: mm) (k–o) total cloud cover (units: %) (p–t) vertical integral of meridional water vapor transport (MIVT; units: kg m^{-1} s^{-1}), and (u–y) height-longitude profile of geopotential height (units: gpm) at the latitudes marked by gray lines in (p–t). Purple contours in (k–o) denote positive 500 hPa geopotential height anomalies (units: gpm), with an interval of 15 gpm in (k, l, m, o) and 5 gpm in (n). Solid (dashed) purple contours in (p–t) denote positive (negative) surface pressure anomalies (units: hPa), with an interval of 1.5 hPa. Gray dots, as well as pink lines hatching in (k–o) and (p–t), indicate the areas where the anomalies are statistically significant at the 95% confidence level. Specifically, gray dots and pink lines hatching in (k–o) represent statistical significance for total cloud cover and 500 hPa geopotential height anomalies, respectively. Gray dots and pink lines hatching in (p–t) represent statistical significance for MIVT and surface pressure anomalies, respectively. Purple lines in (u–y) denote the main longitudes of compound extremes.

Most of the selected WWEs cases, as well as WDEs cases discussed below, share generalized characteristics illustrated by the composite results.

During the WDEs in EU, SC, and USGP, HPs also prevail (Figure 2). However, in contrast to WWEs, WDEs are normally located beneath HPs. When convection is suppressed by downdrafts at the center of HPs, precipitation is reduced (Figures 2h–2j), and clouds are dissipated (Figures 2m–2o). The former process can trigger drought, and the latter creates clear-sky conditions that enhance SWR supply at the surface (Figure 3). Abnormal SWR is absorbed and heats the ground. Then, more energy is lost via upwelling LWR from the surface into the atmosphere (Figures 3r–3t), as well as via surface latent (Figures 3c–3e) and sensible heat fluxes (Figures 3h–3j). Total surface energy differences between WWEs and WDEs indicate that in polar regions, WWEs are driven by anomalous horizontal warm and moist air transport, but in the midlatitude regions, the WDEs are driven by anomalous vertical descending motion.

3.3. Land-Atmosphere Interaction

Larger latent heat flux and sensible heat flux anomalies occur during WDEs over EU, SC, and USGP than during WWEs over GL and WA (Figure 3). Previous studies have suggested that the land-atmosphere interaction significantly contributes to the occurrence of WDEs, particularly to the lengthening of these events (Libonati et al., 2022; Miralles et al., 2019; Seo & Ha, 2022; Zhang et al., 2020). We calculate the coupling metric to

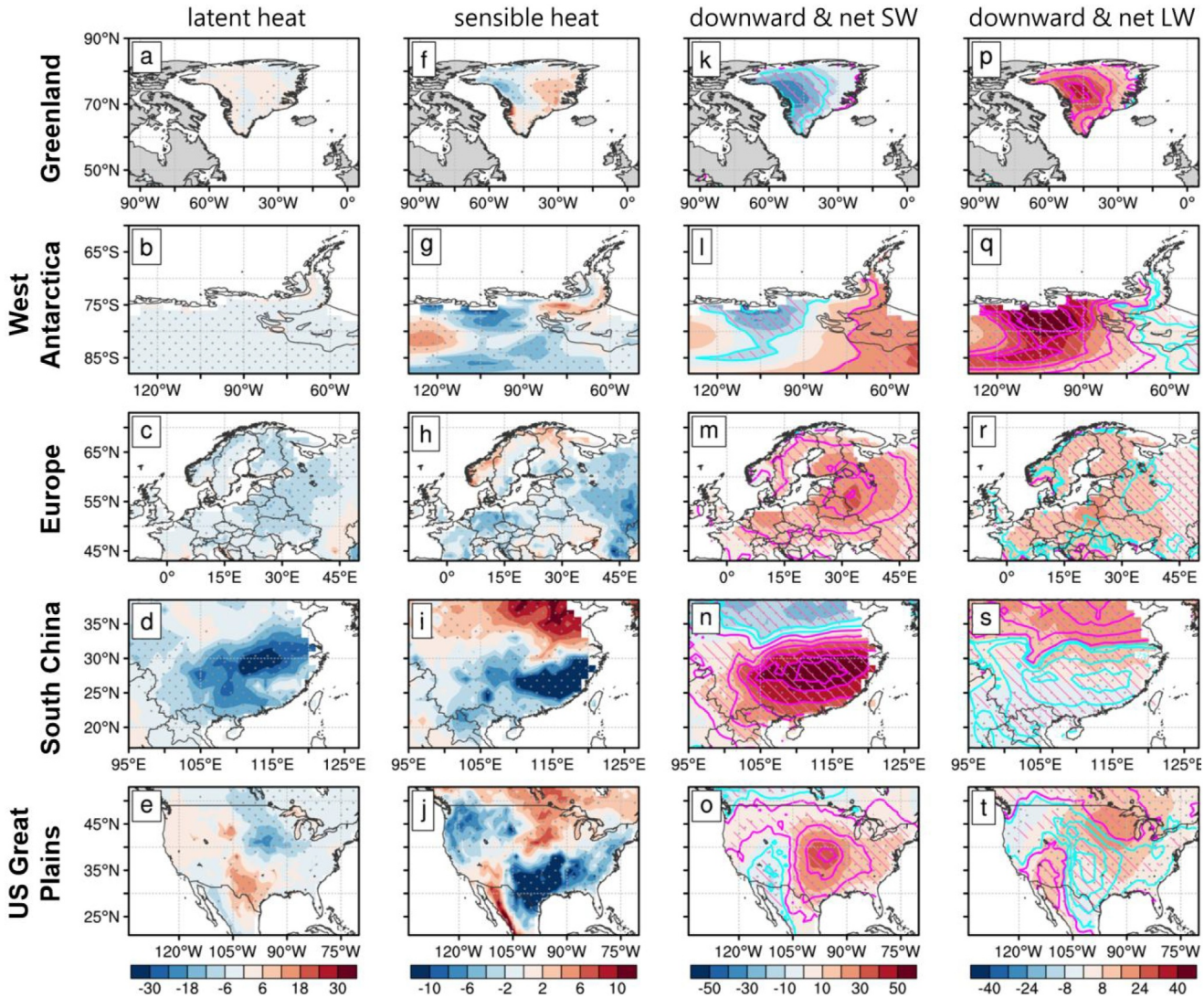

Figure 3. Surface energy budget associated with the WWEs in GL and WA, and the WDEs in EU, SC and USGP. Shading represents daily composite anomaly values of (a–e) latent heat flux (units: W m^{-2}) (f–j) sensible heat flux (units: W m^{-2}) (k–o) downward shortwave radiation (SWR; units: W m^{-2}), and (p–t) downward longwave radiation (LWR; units: W m^{-2}). Pink (blue) contours in (k–o) denote positive (negative) net SWR anomalies (units: W m^{-2}), with an interval of 10 W m^{-2}. Pink (blue) contours in (p–t) denote positive (negative) net LWR anomalies (units: W m^{-2}), with an interval of 5 W m^{-2}. Gray dots, as well as pink lines hatching in (k–o) and (p–t), indicate the areas where the anomalies are statistically significant at the 95% confidence level. Specifically, gray dots and pink lines hatching in (k–o) represent statistical significance for downward SWR and net SWR anomalies, respectively. Gray dots and pink lines hatching in (p–t) represent statistical significance for downward LWR and net LWR anomalies, respectively.

compare the strength of land-atmosphere interaction during WWEs and WDEs. The positive coupling metric over non-ice-covered regions indicates that the land-atmosphere interaction is indeed active during WDEs (Figures 4c–4e). Specifically, under the control of high-pressure systems (HPs), moisture from non-ice-covered surfaces evaporates via adiabatic warming of subsidence motions and excessive downward SWR. These non-ice-covered surfaces can hardly be re-moisturized as precipitation is limited by subsidence motions. Reduced soil moisture (Figures 4h–4j) allows the surface to heat more quickly due to weakened evaporation, and enhances upward sensible heat flux that warms the overlying air. This process further strengthens the existing HPs above, which exacerbates surface dry conditions in turn. Thus, a positive feedback loop to trigger and maintain WDEs is established, explaining why prolonged compound warm extremes tend to occur over non-ice-covered zones.

However, surface turbulent heat fluxes anomalies are negligible over the ice-covered regions. Since deep HPs are commonly thermally maintained, their centers tend to be located above the warmer oceanic surface away from the ice-covered regions, situating the ice sheets on their fringes. As a result, these deep HPs can induce warm-moist

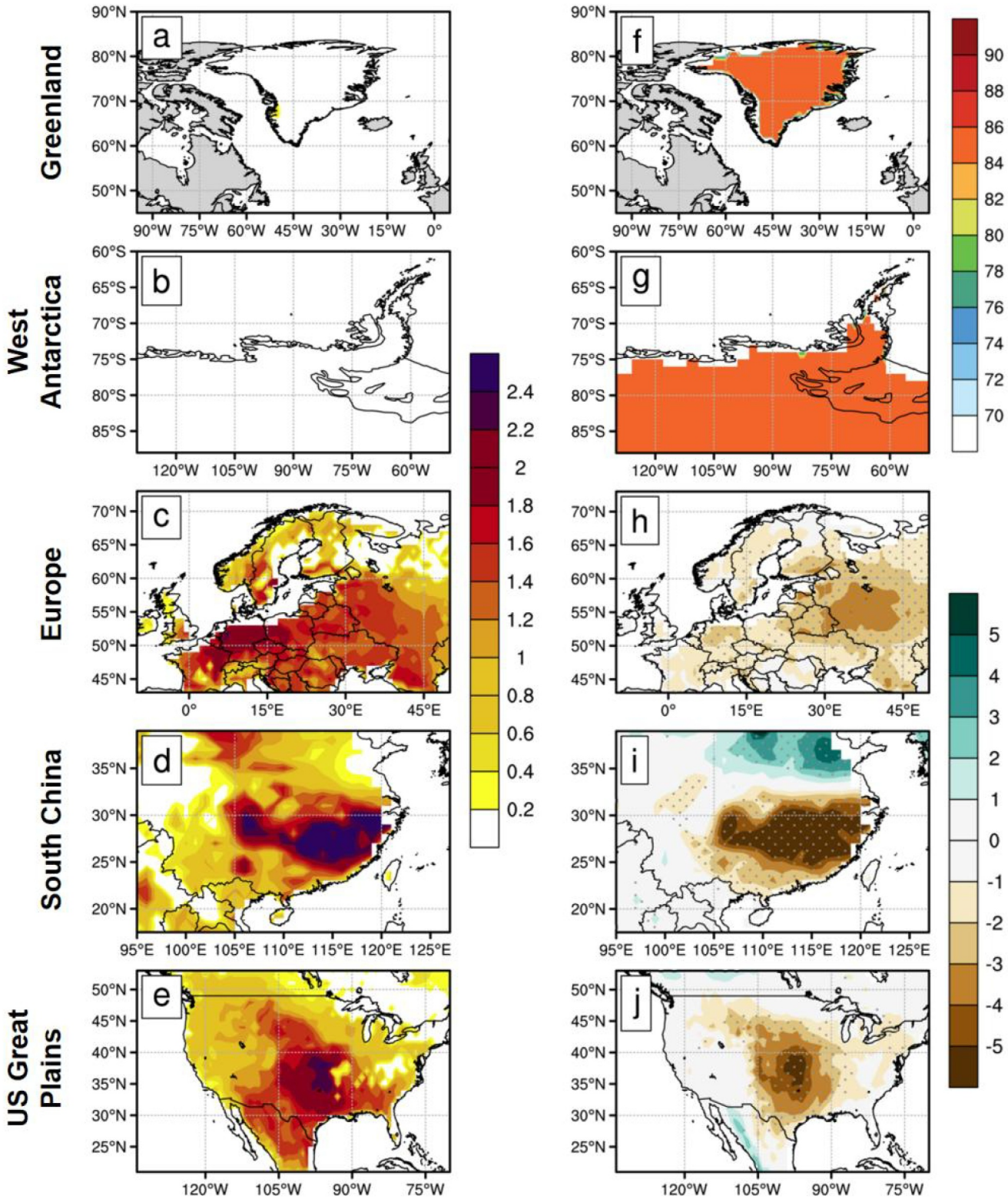

Figure 4. Land-atmosphere interaction associated with the WWEs in GL and WA, and the WDEs in EU, SC and USGP. Shading represents daily composite values of (a–e) coupling metric (f, g) surface albedo (units: %), and (h, i, j) soil moisture anomalies (units: 10^{-2} m^3 m^{-3}). Gray dots indicate the areas where soil moisture anomalies are statistically significant at the 95% confidence level.

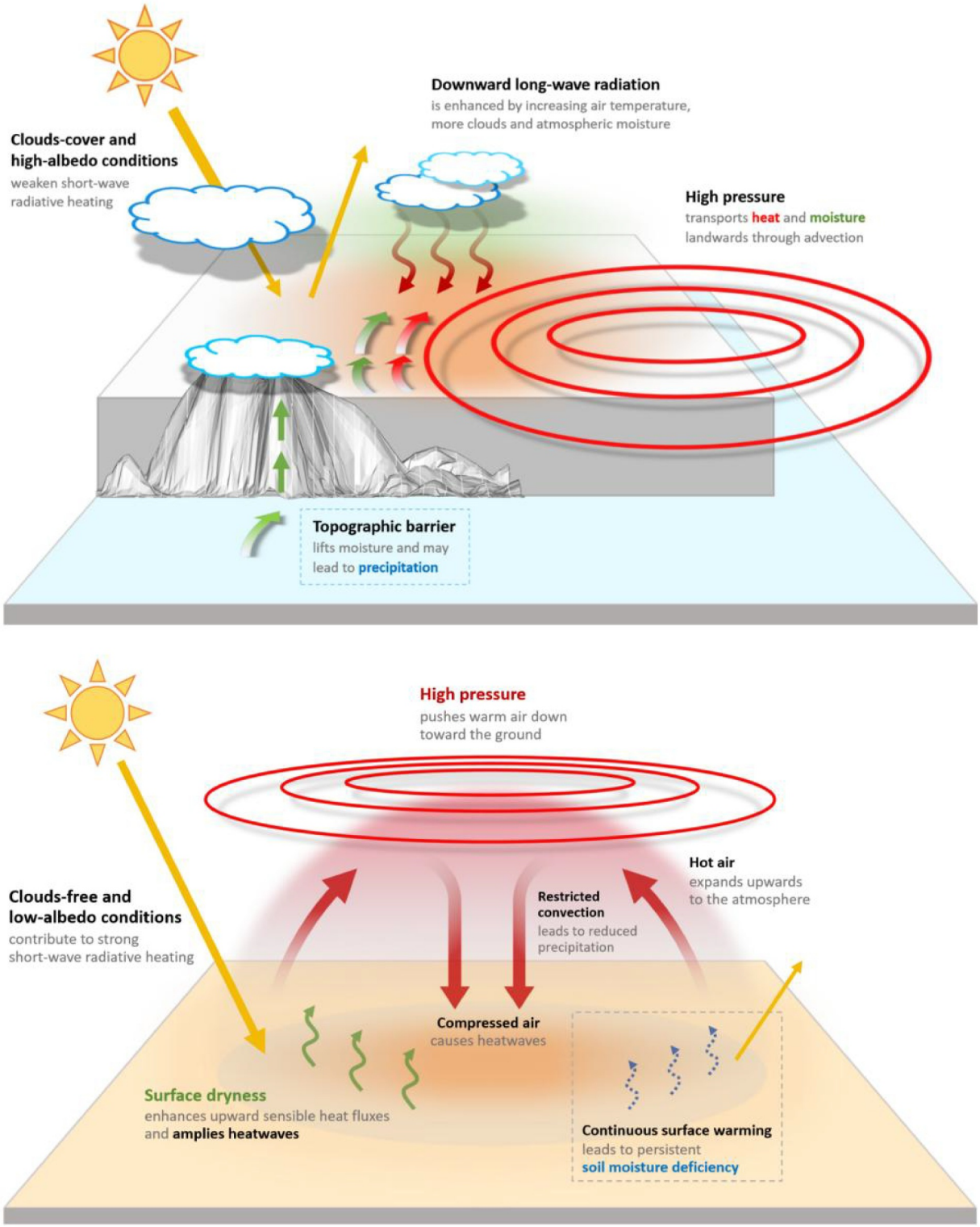

Figure 5. Schematic diagram illustrating the WWEs (top) over the ice-covered surface and the WDEs (bottom) above the non-ice-covered surface.

air intrusions by horizontal advective motions (Pettersen et al., 2022; Vignon et al., 2021) and thus result in the high prevalence of WWEs over the polar ice sheets. All the aforementioned local dynamic processes and surface energy responses controlled by HPs during WWEs and WDEs are summarized in the schematic diagram as shown in Figure 5.

4. Conclusions

In this study, we reveal the physical mechanisms for paradigm differences of compound warm extremes between midlatitude regions and ice-covered polar regions. Warm-wet extremes (WWEs) and warm-dry extremes (WDEs), the two different types of compound warm extremes, are defined by the joint percentile thresholds of 2 m temperature and precipitation. WDEs, which typically last longer and prevail in non-ice-covered zones, differ substantially from WWEs, which exhibit shorter durations and exist predominantly in ice-covered regions. Both WWEs and WDEs are driven by anomalous high-pressure systems (HPs), but they experience distinct local dynamic processes. By comparing the physical mechanisms for compound warm extremes in Greenland, West Antarctica, Europe, South China, and the US Great Plains, we conclude that the paradigm differences result from a combination of attenuation in land-atmosphere interaction and transformation in the dynamic processes controlled by HPs.

Since the dynamics responsible for the WDEs are consistent with previous studies (Libonati et al., 2022; Miralles et al., 2014, 2019; Zhang et al., 2023), we specifically focus on WWEs-related local dynamic processes and land-air interaction created by HPs in ice-covered regions. WWEs over ice sheets are sustained by horizontal warm and moist air intrusions. When warm air encounters the ice sheet, the surface is directly warmed by longwave radiation, while the air cools down, leading to increased cloud cover. The abundant clouds can trap more longwave radiation between the surface and the clouds due to their longwave effect but reduce shortwave radiation to the surface. Simultaneously, more clouds over the ice sheet can lead to more precipitation. These physical processes are responsible for the high prevalence of WWEs in polar regions. Specifically, the ice cover acts as a barrier that dampens land-atmosphere interaction, resulting in a relatively shorter duration of WWEs.

An improved understanding of WWEs over polar regions would enable us to make more accurate projections of climate changes in these regions and assess relative climate risks. Under the background of global climate change, precipitation during WWEs over the ice sheet tends to change from snowfall to rainfall (Xu et al., 2022). Unlike snowfall, rainfall can directly infiltrate the ice sheet, leading to enhanced surface melting and potential destabilization (Box et al., 2022; Dou et al., 2023) and posing a larger threat from WWEs to the ice sheet (Bennartz et al., 2013; Schot et al., 2023; Vignon et al., 2021). In this study, we present the climatological characteristics of WWEs. However, several important questions remain, including trends and variability of WWEs' characteristics (i.e., intensity, duration, and spatial extent) and their associated climate impacts, which need to be studied in future research. Additionally, the duration of WWEs ranges from less than 3 days to more than 15 days, indicating significant differences among individual cases. Therefore, more attention should be given to the diversity in the evolution of WWEs. These would be beneficial for making more accurate projections of changes in polar ice sheets and for taking proactive measures to mitigate the potential consequence on polar ice sheets.

Data Availability Statement

The pressure-levels and single-levels ERA5 reanalysis data used in the study are publicly available at Copernicus Climate Change Service (C3S) Climate Data Store (CDS) via Hersbach et al. (2023a, 2023b), respectively.

Acknowledgments
We would like to express our heartfelt gratitude to the editor and the two anonymous reviewers for their invaluable and constructive comments. Their comprehensive, insightful, and instructive feedback significantly leads to substantial improvement of the manuscript. This research is supported by the Guangdong Major Project of Basic and Applied Basic Research (2020B0301030004) and the National Natural Science Foundation of China (42075028).

References

Afroz, M., Chen, G., & Anandhi, A. (2023). Drought- and heatwave-associated compound extremes: A review of hotspots, variables, parameters, drivers, impacts, and analysis frameworks. *Frontiers in Earth Science*, *10*, 914437. https://doi.org/10.3389/feart.2022.914437

Bakker, P., Schmittner, A., Lenaerts, J. T. M., Abe-Ouchi, A., Bi, D., Van Den Broeke, M. R., et al. (2016). Fate of the atlantic meridional overturning circulation: Strong decline under continued warming and Greenland melting. *Geophysical Research Letters*, *43*(23). https://doi.org/10.1002/2016GL070457

Barrett, B. S., Henderson, G. R., McDonnell, E., Henry, M., & Mote, T. (2020). Extreme Greenland blocking and high-latitude moisture transport. *Atmospheric Science Letters*, *21*(11), e1002. https://doi.org/10.1002/asl.1002

Barriopedro, D., García-Herrera, R., Ordóñez, C., Miralles, D. G., & Salcedo-Sanz, S. (2023). Heat waves: Physical understanding and scientific challenges. *Reviews of Geophysics*, *61*(2), e2022RG000780. https://doi.org/10.1029/2022RG000780

Bell, R. E., Banwell, A. F., Trusel, L. D., & Kingslake, J. (2018). Antarctic surface hydrology and impacts on ice-sheet mass balance. *Nature Climate Change*, *8*(12), 1044–1052. https://doi.org/10.1038/s41558-018-0326-3

Beniston, M. (2009). Trends in joint quantiles of temperature and precipitation in Europe since 1901 and projected for 2100. *Geophysical Research Letters*, *36*(7), 2008GL037119. https://doi.org/10.1029/2008GL037119

Bennartz, R., Shupe, M. D., Turner, D. D., Walden, V. P., Steffen, K., Cox, C. J., et al. (2013). 2012 Greenland melt extent enhanced by low-level liquid clouds. *Nature*, *496*(7443), 83–86. https://doi.org/10.1038/nature12002

Bintanja, R. (2018). The impact of Arctic warming on increased rainfall. *Scientific Reports*, *8*(1), 16001. https://doi.org/10.1038/s41598-018-34450-3

Bintanja, R., Graversen, R. G., & Kolbe, M. (2023). Regional polar warming linked to poleward moisture transport variability. *Environmental Research: Climate*, *2*(4), 041003. https://doi.org/10.1088/2752-5295/acee9e

Box, J. E., Wehrlé, A., van As, D., Fausto, R. S., Kjeldsen, K. K., Dachauer, A., et al. (2022). Greenland ice sheet rainfall, heat and albedo feedback impacts from the mid-August 2021 atmospheric river. *Geophysical Research Letters*, *49*(11), e2021GL097356. https://doi.org/10.1029/2021GL097356

Bozkurt, D., Marín, J. C., & Barrett, B. S. (2022). Temperature and moisture transport during atmospheric blocking patterns around the Antarctic Peninsula. *Weather and Climate Extremes*, *38*, 100506. https://doi.org/10.1016/j.wace.2022.100506

Cai, Z., You, Q., Chen, H. W., Zhang, R., Zuo, Z., Chen, D., et al. (2024). Assessing Arctic wetting: Performances of CMIP6 models and projections of precipitation changes. *Atmospheric Research*, *297*, 107124. https://doi.org/10.1016/j.atmosres.2023.107124

Clem, K. R., Adusumilli, S., Baiman, R., Banwell, A. F., Barreira, S., Beadling, R. L., et al. (2023). Antarctica and the southern ocean. *Bulletin of the American Meteorological Society*, *104*(9), S322–S365. https://doi.org/10.1175/BAMS-D-23-0077.1

Deb, P., Orr, A., Hosking, J. S., Phillips, T., Turner, J., Bannister, D., et al. (2016). An assessment of the Polar Weather Research and Forecasting (WRF) model representation of near-surface meteorological variables over West Antarctica. *Journal of Geophysical Research: Atmospheres*, *121*(4), 1532–1548. https://doi.org/10.1002/2015JD024037

DeConto, R. M., & Pollard, D. (2016). Contribution of Antarctica to past and future sea-level rise. *Nature*, *531*(7596), 591–597. https://doi.org/10.1038/nature17145

Djoumna, G., & Holland, D. M. (2021). Atmospheric rivers, warm air intrusions, and surface radiation balance in the Amundsen Sea Embayment. *Journal of Geophysical Research: Atmospheres*, *126*(13), e2020JD034119. https://doi.org/10.1029/2020JD034119

Dou, T., Xie, Z., Box, J., Yang, Q., Yang, Y., Teng, S., et al. (2023). Analysis of the record-breaking August 2021 rainfall over the Greenland ice sheet. *Advances in Polar Science*, *34*(3), 165–176. 2023. https://doi.org/10.12429/j.advps.2022.0016

Feng, S., Hao, Z., Zhang, X., & Hao, F. (2019). Probabilistic evaluation of the impact of compound dry-hot events on global maize yields. *Science of the Total Environment*, *689*, 1228–1234. https://doi.org/10.1016/j.scitotenv.2019.06.373

Feron, S., Cordero, R. R., Damiani, A., Malhotra, A., Seckmeyer, G., & Llanillo, P. (2021). Warming events projected to become more frequent and last longer across Antarctica. *Scientific Reports*, *11*(1), 19564. https://doi.org/10.1038/s41598-021-98619-z

Gao, Y., Liu, J., Wen, Q., Chen, D., Sun, W., Ning, L., & Yan, M. (2024). The influence of increased CO_2 concentrations on AMOC interdecadal variability under the LGM background. *Journal of Geophysical Research: Atmospheres*, *129*(3), e2023JD039976. https://doi.org/10.1029/2023JD039976

González-Herrero, S., Barriopedro, D., Trigo, R. M., López-Bustins, J. A., & Oliva, M. (2022). Climate warming amplified the 2020 record-breaking heatwave in the Antarctic Peninsula. *Communications Earth & Environment*, *3*(1), 1–9. https://doi.org/10.1038/s43247-022-00450-5

Gorodetskaya, I. V., Durán-Alarcón, C., González-Herrero, S., Clem, K. R., Zou, X., Rowe, P., et al. (2023). Record-high antarctic Peninsula temperatures and surface melt in february 2022: A compound event with an intense atmospheric river. *Npj Climate and Atmospheric Science*, *6*(1), 202. https://doi.org/10.1038/s41612-023-00529-6

Han, Q., Xu, W., & Shi, P. (2022). Mapping global population exposure to heatwaves. In *Atlas of global change risk of population and economic systems* (pp. 95–102). Springer Nature. https://doi.org/10.1007/978-981-16-6691-9_6

Hao, Z., Hao, F., Singh, V. P., Xia, Y., Shi, C., & Zhang, X. (2018). A multivariate approach for statistical assessments of compound extremes. *Journal of Hydrology*, *565*, 87–94. https://doi.org/10.1016/j.jhydrol.2018.08.025

Hao, Z., Hao, F., Xia, Y., Feng, S., Sun, C., Zhang, X., et al. (2022). Compound droughts and hot extremes: Characteristics, drivers, changes, and impacts. *Earth-Science Reviews*, *235*, 104241. https://doi.org/10.1016/j.earscirev.2022.104241

He, Y., Fang, J., Xu, W., & Shi, P. (2022). Substantial increase of compound droughts and heatwaves in wheat growing seasons worldwide. *International Journal of Climatology*, *42*(10), 5038–5054. https://doi.org/10.1002/joc.7518

Hersbach, H., Bell, B., Berrisford, P., Biavati, G., Horányi, A., Muñoz Sabater, J., et al. (2023a). ERA5 hourly data on pressure levels from 1940 to present. [Dataset]. https://doi.org/10.24381/cds.bd0915c6. *Copernicus Climate Change Service (C3S) Climate Data Store (CDS)*.

Hersbach, H., Bell, B., Berrisford, P., Biavati, G., Horányi, A., Muñoz Sabater, J., et al. (2023b). ERA5 hourly data on single levels from 1940 to present. [Dataset]. https://doi.org/10.24381/cds.adbb2d47. *Copernicus Climate Change Service (C3S) Climate Data Store (CDS)*.

Hersbach, H., Bell, B., Berrisford, P., Hirahara, S., Horányi, A., Muñoz-Sabater, J., et al. (2020). The ERA5 global reanalysis. *Quarterly Journal of the Royal Meteorological Society*, *146*(730), 1999–2049. https://doi.org/10.1002/qj.3803

Holmes, A., Rüdiger, C., Mueller, B., Hirschi, M., & Tapper, N. (2017). Variability of soil moisture proxies and hot days across the climate regimes of Australia. *Geophysical Research Letters*, *44*(14), 7265–7275. https://doi.org/10.1002/2017GL073793

Hu, X., Sejas, S. A., Cai, M., Li, Z., & Yang, S. (2019). Atmospheric dynamics footprint on the January 2016 ice sheet melting in West Antarctica. *Geophysical Research Letters*, *46*(5), 2829–2835. https://doi.org/10.1029/2018GL081374

Jiang, N., Zhu, C., Hu, Z.-Z., McPhaden, M. J., Chen, D., Liu, B., et al. (2024). Enhanced risk of record-breaking regional temperatures during the 2023–24 El Niño. *Scientific Reports*, *14*(1), 2521. https://doi.org/10.1038/s41598-024-52846-2

Leeson, A. A., Eastoe, E., & Fettweis, X. (2018). Extreme temperature events on Greenland in observations and the MAR regional climate model. *The Cryosphere*, *12*(3), 1091–1102. https://doi.org/10.5194/tc-12-1091-2018

Li, W., Wu, Y., & Hu, X. (2023). The processes-based attributes of four major surface melting events over the Antarctic Ross ice shelf. *Advances in Atmospheric Sciences*, *40*(9), 1662–1670. https://doi.org/10.1007/s00376-023-2287-3

Libonati, R., Geirinhas, J. L., Silva, P. S., Russo, A., Rodrigues, J. A., Belém, L. B. C., et al. (2022). Assessing the role of compound drought and heatwave events on unprecedented 2020 wildfires in the Pantanal. *Environmental Research Letters*, *17*(1), 015005. https://doi.org/10.1088/1748-9326/ac462e

Liu, Z., & Zhou, W. (2023a). Global seasonal-scale meteorological droughts. Part I: Detection, metrics, and inland/coastal types. *Ocean-Land-Atmosphere Research*, *2*, 0016. https://doi.org/10.34133/olar.0016

Liu, Z., & Zhou, W. (2023b). Global seasonal-scale meteorological droughts. Part II: Temperature anomaly-based classifications. *Ocean-Land-Atmosphere Research*, *2*, 0017. https://doi.org/10.34133/olar.0017

Mattingly, K. S., Mote, T. L., Fettweis, X., van As, D., Tricht, K. V., Lhermitte, S., et al. (2020). Strong summer atmospheric rivers trigger Greenland ice sheet melt through spatially varying surface energy balance and cloud regimes. *Journal of Climate*, *33*(16), 6809–6832. https://doi.org/10.1175/JCLI-D-19-0835.1

McNeall, D., Halloran, P. R., Good, P., & Betts, R. A. (2011). Analyzing abrupt and nonlinear climate changes and their impacts. *WIREs Climate Change*, *2*(5), 663–686. https://doi.org/10.1002/wcc.130

Miralles, D. G., Gentine, P., Seneviratne, S. I., & Teuling, A. J. (2019). Land–atmospheric feedbacks during droughts and heatwaves: State of the science and current challenges. *Annals of the New York Academy of Sciences*, *1436*(1), 19–35. https://doi.org/10.1111/nyas.13912

Miralles, D. G., Teuling, A. J., van Heerwaarden, C. C., & Vilà-Guerau de Arellano, J. (2014). Mega-heatwave temperatures due to combined soil desiccation and atmospheric heat accumulation. *Nature Geoscience*, *7*(5), 345–349. https://doi.org/10.1038/ngeo2141

Miralles, D. G., Van Den Berg, M. J., Teuling, A. J., & De Jeu, R. A. M. (2012). Soil moisture-temperature coupling: A multiscale observational analysis. *Geophysical Research Letters*, *39*(21), 2012GL053703. https://doi.org/10.1029/2012GL053703

Mueller, B., & Seneviratne, S. I. (2012). Hot days induced by precipitation deficits at the global scale. *Proceedings of the National Academy of Sciences*, *109*(31), 12398–12403. https://doi.org/10.1073/pnas.1204330109

Mukherjee, S., Ashfaq, M., & Mishra, A. K. (2020). Compound drought and heatwaves at a global scale: The role of natural climate variability-associated synoptic patterns and land-surface energy budget anomalies. *Journal of Geophysical Research: Atmospheres*, *125*(11), e2019JD031943. https://doi.org/10.1029/2019JD031943

Nicolas, J. P., & Bromwich, D. H. (2011). Climate of West Antarctica and influence of marine air intrusions. *Journal of Climate*, *24*(1), 49–67. https://doi.org/10.1175/2010JCLI3522.1

Pettersen, C., Henderson, S. A., Mattingly, K. S., Bennartz, R., & Breeden, M. L. (2022). The critical role of Euro-Atlantic blocking in promoting snowfall in central Greenland. *Journal of Geophysical Research: Atmospheres*, *127*(6), e2021JD035776. https://doi.org/10.1029/2021JD035776

Ridder, N. N., Pitman, A. J., & Ukkola, A. M. (2021). Do CMIP6 climate models simulate global or regional compound events skillfully? *Geophysical Research Letters*, *48*(2), e2020GL091152. https://doi.org/10.1029/2020GL091152

Ridder, N. N., Pitman, A. J., Westra, S., Ukkola, A., Do, H. X., Bador, M., et al. (2020). Global hotspots for the occurrence of compound events. *Nature Communications*, *11*(1), 5956. https://doi.org/10.1038/s41467-020-19639-3

Rignot, E., Velicogna, I., Van Den Broeke, M. R., Monaghan, A., & Lenaerts, J. T. M. (2011). Acceleration of the contribution of the Greenland and Antarctic ice sheets to sea level rise: Acceleration of ice sheet loss. *Geophysical Research Letters*, *38*(5), n/a-n–a. https://doi.org/10.1029/2011GL046583

Salvador, C., Nieto, R., Vicente-Serrano, S. M., García-Herrera, R., Gimeno, L., & Vicedo-Cabrera, A. M. (2023). Public health implications of drought in a climate change context: A critical review. *Annual Review of Public Health*, *44*(1), 213–232. https://doi.org/10.1146/annurev-publhealth-071421-051636

Seo, Y.-W., & Ha, K.-J. (2022). Changes in land-atmosphere coupling increase compound drought and heatwaves over northern East Asia. *Npj Climate and Atmospheric Science*, *5*(1), 100. https://doi.org/10.1038/s41612-022-00325-8

Shields, C. A., Wille, J. D., Marquardt Collow, A. B., Maclennan, M., & Gorodetskaya, I. V. (2022). Evaluating uncertainty and modes of variability for Antarctic atmospheric rivers. *Geophysical Research Letters*, *49*(16), e2022GL099577. https://doi.org/10.1029/2022GL099577

Stokes, C. R., Abram, N. J., Bentley, M. J., Edwards, T. L., England, M. H., Foppert, A., et al. (2022). Response of the east antarctic ice sheet to past and future climate change. *Nature*, *608*(7922), 275–286. https://doi.org/10.1038/s41586-022-04946-0

Tripathy, K. P., & Mishra, A. K. (2023). How unusual is the 2022 European compound drought and heatwave event? *Geophysical Research Letters*, *50*(15), e2023GL105453. https://doi.org/10.1029/2023GL105453

van der Schot, J., Abermann, J., Silva, T., Jensen, C. D., Noël, B., & Schöner, W. (2023). Precipitation trends (1958–2021) on Ammassalik island, south-east Greenland. *Frontiers in Earth Science*, *10*. https://doi.org/10.3389/feart.2022.1085499

Vignon, É., Roussel, M.-L., Gorodetskaya, I. V., Genthon, C., & Berne, A. (2021). Present and future of rainfall in Antarctica. *Geophysical Research Letters*, *48*(8), e2020GL092281. https://doi.org/10.1029/2020GL092281

Wang, S., Ding, M., Liu, G., Zhao, S., Zhang, W., Li, X., et al. (2023). New record of explosive warmings in East Antarctica. *Science Bulletin*, *68*(2), 129–132. https://doi.org/10.1016/j.scib.2022.12.013

Ward, J. L., Flanner, M. G., & Dunn-Sigouin, E. (2020). Impacts of Greenland block location on clouds and surface energy fluxes over the Greenland ice sheet. *Journal of Geophysical Research: Atmospheres*, *125*(22), e2020JD033172. https://doi.org/10.1029/2020JD033172

Wille, J. D., Alexander, S. P., Amory, C., Baiman, R., Barthélemy, L., Bergstrom, D. M., et al. (2024). The extraordinary March 2022 East Antarctica "heat" wave. Part II: Impacts on the Antarctic ice sheet. *Journal of Climate*, *37*(3), 779–799. https://doi.org/10.1175/JCLI-D-23-0176.1

Xu, L., Zhang, T., Yu, W., & Yang, S. (2023). Changes in concurrent precipitation and temperature extremes over the Asian monsoon region: Observation and projection. *Environmental Research Letters*, *18*(4), 044021. https://doi.org/10.1088/1748-9326/acbfd0

Xu, M., Yang, Q., Hu, X., Liang, K., & Vihma, T. (2022). Record-breaking rain falls at Greenland summit controlled by warm moist-air intrusion. *Environmental Research Letters*, *17*(4), 044061. https://doi.org/10.1088/1748-9326/ac60d8

Yang, R., Hu, X., Cai, M., Deng, Y., Clem, K., Yang, S., et al. (2024). A paradigm shift of compound extremes over polar ice sheets. *Ocean-Land-Atmosphere Research*, *3*, 0040. https://doi.org/10.34133/olar.0040

Yang, X., Shen, C., Zhang, G., & Chen, D. (2024). Enhanced spring warming of the Tibetan Plateau amplifies summer heat stress in eastern Europe. *Climate Dynamics*. https://doi.org/10.1007/s00382-024-07197-z

Yang, X., Zeng, G., Zhang, S., Iyakaremye, V., Shen, C., Wang, W.-C., & Chen, D. (2024). Phase-locked Rossby wave-4 pattern dominates the 2022-like concurrent heat extremes across the Northern Hemisphere. *Geophysical Research Letters*, *51*(4), e2023GL107106. https://doi.org/10.1029/2023GL107106

Zhang, P., Jeong, J.-H., Yoon, J.-H., Kim, H., Wang, S.-Y. S., Linderholm, H. W., et al. (2020). Abrupt shift to hotter and drier climate over inner East Asia beyond the tipping point. *Science*, *370*(6520), 1095–1099. https://doi.org/10.1126/science.abb3368

Zhang, T., Deng, Y., Chen, J., Yang, S., & Dai, Y. (2023). An energetics tale of the 2022 mega-heatwave over central-eastern China. *Npj Climate and Atmospheric Science*, *6*(1), 162. https://doi.org/10.1038/s41612-023-00490-4

Zhu, J., Liu, Z., Zhang, X., Eisenman, I., & Liu, W. (2014). Linear weakening of the AMOC in response to receding glacial ice sheets in CCSM3. *Geophysical Research Letters*, *41*(17), 6252–6258. https://doi.org/10.1002/2014GL060891

Zou, X., Bromwich, D. H., Montenegro, A., Wang, S., & Bai, L. (2021). Major surface melting over the ross ice shelf. Part I: Foehn effect. *Quarterly Journal of the Royal Meteorological Society*, *147*(738), 2874–2894. https://doi.org/10.1002/qj.4104

Zscheischler, J., & Seneviratne, S. I. (2017). Dependence of drivers affects risks associated with compound events. *Science Advances*, *3*(6), e1700263. https://doi.org/10.1126/sciadv.1700263